JACS
JOURNAL OF THE AMERICAN CHEMICAL SOCIETY

Communication

pubs.acs.org/JACS

Deep-UV Surface-Enhanced Resonance Raman Scattering of Adenine on Aluminum Nanoparticle Arrays

Shankar K. Jha,*[,†] Zeeshan Ahmed,[†,∥] Mario Agio,[‡] Yasin Ekinci,*[,†,§] and Jörg F. Löffler[†]

[†]Laboratory of Metal Physics and Technology, Department of Materials, ETH Zürich, 8093 Zürich, Switzerland

[‡]Laboratory of Physical Chemistry, ETH Zürich, 8093 Zürich, Switzerland

[§]Laboratory for Micro- and Nanotechnology, Paul Scherrer Institute, 5232 Villigen-PSI, Switzerland

Supporting Information

ABSTRACT: We report the ultrasensitive detection of adenine using deep-UV surface-enhanced resonance Raman scattering on aluminum nanostructures. Well-defined Al nanoparticle arrays fabricated over large areas using extreme-UV interference lithography exhibited sharp and tunable plasmon resonances in the UV and deep-UV wavelength ranges. Theoretical modeling based on the finite-difference time-domain method was used to understand the near-field and far-field optical properties of the nanoparticle arrays. Raman measurements were performed on adenine molecules coated uniformly on the Al nanoparticle arrays at a laser excitation wavelength of 257.2 nm. With this technique, less than 10 amol of label-free adenine molecules could be detected reproducibly in real time. Zeptomole (~30 000 molecules) detection sensitivity was readily achieved proving that deep-UV surface-enhanced resonance Raman scattering is an extremely sensitive tool for the detection of biomolecules.

Raman spectroscopy is an important analytical technique that provides information about molecular bonds on the basis of their unique vibrational signatures. However, its application at low analyte concentrations is limited by the inherently low Raman cross sections (typically 10^{-31}–10^{-29} cm^2/molecule).[1] Surface-enhanced Raman scattering (SERS) has emerged as an important technique for enhancing the Raman scattering cross section. Here, enhancement of the electromagnetic (EM) field at the metal nanoparticle surface due to the excitation of localized surface plasmon resonance (LSPR) in a metal nanostructure is considered to be the dominant SERS enhancement mechanism.[2−4] Molecules on the metal surface or in close proximity to it experience the increased EM near-field and therefore scatter more efficiently. With recent advancements in the fabrication of metal nanostructures and improved detection techniques, SERS has emerged as a technique capable of ultrasensitive detection down to a single molecule.[5−7] However, for realization of practical SERS-based sensors for quantitative and real-time applications, the high sensitivity and specificity of this technique must be accompanied by controlled and high-throughput fabrication techniques and reproducible and, preferably, label-free detection schemes.

Since the Raman scattering cross-section scales with the fourth power of the excitation frequency (ω^4),[1] UV and deep-UV (DUV) excitations have long been utilized to extend the application of Raman spectroscopy to many organic and inorganic molecules that have small Raman cross sections in the visible and near-IR (NIR) regions.[8] Furthermore, with DUV excitation, the fluorescence and Raman bands are well-separated which leads to a fluorescence-free background and thus boosts the signal-to-noise ratio (SNR) of the Raman spectra.[9] Additionally, many important biomolecules, such as proteins and DNA, have their electronic absorption bands in the DUV region, resulting in a resonance Raman (RR) effect that provides up to 10^8-fold enhancement of the Raman cross section.[10] Such a large enhancement combined with the high molecular specificity of the RR process has been gainfully exploited for highly sensitive biophysical studies on complex biomolecules.[11−13] Combining the advantages of both SERS and DUV-RR phenomena, DUV surface-enhanced RR spectroscopy (DUV-SERRS) has great potential for ultrasensitive and highly specific biomolecular detection.

SERS studies are generally limited to the visible and NIR regions because the commonly used noble-metal substrates support strong plasmon resonances at these wavelengths.[2−4] The EM enhancements exhibited by these substrates are very small in the UV and DUV because of damping caused by the interband transitions.[14] UV-excited SERS studies[15−19] were explored on transition metals such as Pd and Rh with limited success. In contrast, Al, which has a low absorption down to 200 nm,[14] is a promising plasmonic material in the UV and DUV wavelength ranges. Although it is well-known that a relatively stable natural oxide layer of 2−5 nm thickness is formed on its surface,[20] Al nanostructures have been shown to exhibit strong plasmon resonances at wavelengths ranging from DUV to NIR.[20−24] Surface-enhanced fluorescence (SEF)[25] and SERS[26] on rough Al surfaces and tip-enhanced Raman scattering (TERS)[27] using Al tips have been demonstrated in the UV and DUV wavelength ranges. Theoretical calculations[28−30] have indicated that high enhancement factors (EFs) can be achieved using Al nanostructures.

In this communication, we report DUV-SERRS of adenine molecules on fabricated Al nanostructures. The Al nanoparticle arrays were fabricated using extreme-UV interference lithography (EUV-IL). This method enables the fabrication of periodic nanostructures over large areas with sub-10 nm

Received: November 7, 2011
Published: January 5, 2012

dx.doi.org/10.1021/ja210446w | J. Am. Chem.Soc. 2012, 134, 1966−1969

resolution and high throughput.[31] We fabricated various Al nanoparticle arrays with a particle height of 70 nm and diameters varying from 65 to 140 nm in a square lattice with a periodicity of 200 nm [see the Supporting Information (SI)]. As shown in Figure 1a,b, the nanoparticles were highly uniform

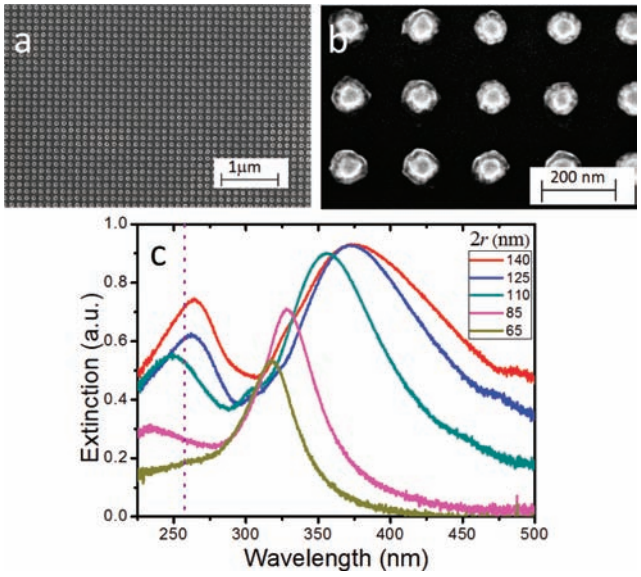

Figure 1. (a) Large-area scanning electron microscopy image of a typical Al nanoparticle array. (b) Magnified image of the nanoparticle array. (c) Far-field optical extinction spectra of nanoparticle arrays having a height of 70 nm, periodicity of 200 nm, and various particle diameters ($2r$). The vertical dashed line indicates the laser excitation wavelength (257.2 nm).

over the fabricated area (400 μm × 400 μm). Individual particles exhibited a tapered-cylinder morphology with a diminution angle of ~12°, as deduced from measurements of the top and bottom diameters of the nanoparticles. An UV optical setup was developed (see the SI) for LSPR and Raman measurements.

The extinction spectra of the Al nanoparticle arrays with various nanoparticle diameters ($2r$) are shown in Figure 1c. We observed these arrays to exhibit two strong plasmon resonances within the measured wavelength range. The resonance peaks at ~350 and ~250 nm are attributed to the dipolar and quadrupolar plasmon modes, respectively. As the particle size increased, there was a general red-shift and broadening of the resonance peaks along with an increase in the corresponding extinction coefficient. Our results clearly demonstrate that tunable and sharp plasmon resonances can be achieved in the UV and DUV regions using Al nanoparticle arrays.

Adenine, a thoroughly studied Raman-active biomolecule, was chosen as the analyte for DUV-SERRS measurements because it has a strong absorption band in the DUV close to the excitation wavelength of 257.2 nm. As indicated in Figure 1c, the laser excitation coincides with the quadrupolar resonance of the nanoparticle arrays. Although the dipolar resonance modes might lead to higher SERS enhancement, these modes are in the blue and near-UV wavelength region, where the advantages of DUV excitation would not be accessible. The samples were prepared by sublimating adenine (99% purity, Sigma-Aldrich) on the Al nanoparticle arrays under high vacuum (~3×10^{-6} mbar). Often-used techniques for analyte deposition such as dip-coating, drop-coating, and spin-coating generally produce inhomogeneous analyte distributions unless appropriate functionalization methods are used. Sublimation, on the other hand, allows for uniform deposition of known amounts of analyte on the substrate surface and therefore enables quantitative spectroscopic measurements. The sublimation temperature used was ~180 °C, which is far below the melting temperature of adenine at atmospheric pressure (360 °C). The film thickness was monitored in situ by a calibrated quartz crystal microbalance. The absorption spectra of adenine films deposited on fused silica substrates (see the SI) indicated that the familiar liquid-phase absorption band of adenine at 260 nm[32−34] was red-shifted to ~272 nm in accordance with previous studies.[35] The presence of this absorption band clearly indicates that we were able to deposit adenine without any significant thermal degradation. Furthermore, absorption measurements performed over different parts of the sublimated films gave rise to similar absorption values, indicating that the deposited film had a uniform thickness.

The Raman spectra of 1 nm thick films of adenine deposited on a bare substrate and on an Al nanoparticle array are presented in Figure 2a. We observed a clear enhancement in

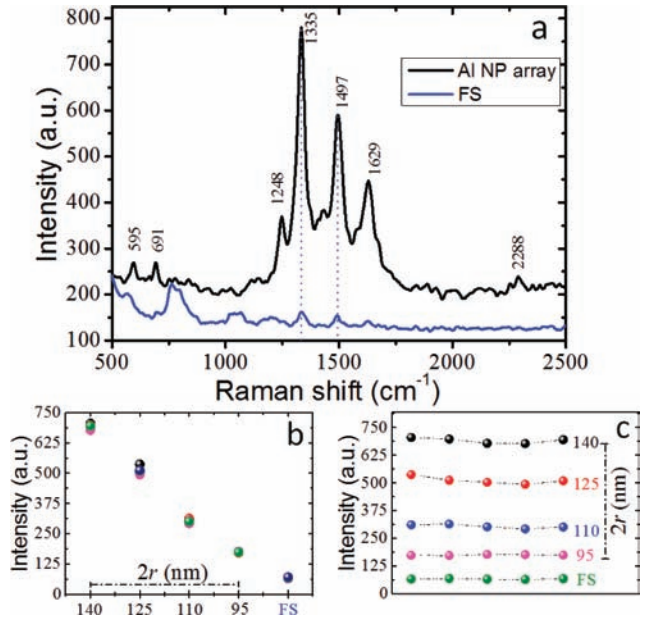

Figure 2. (a) Raman spectra of a 1 nm thick adenine film deposited on fused silica (FS) and on an Al nanoparticle array with $2r$ = 140 nm. The signal collection time was 1 s. (b) Intensity of the 1335 cm^{-1} Raman band plotted against the nanoparticle diameter. (c) Peak intensities of the 1335 cm^{-1} adenine band at different positions on FS and on Al nanoparticle arrays with various particle diameters.

the Raman signal from adenine on the Al nanoparticle substrate. With an incident power of 0.65 mW and a signal integration time of 1 s, the intensity of the RR spectrum is barely discernible over the prevailing background noise. In contrast, the SERRS peaks are clearly distinguishable, with an SNR of ~50. We note that in the SERRS-enhanced spectra, only the Raman bands around 1335 cm^{-1} are selectively enhanced at this excitation, whereas in SERS experiments in the visible range, the adenine band at 730 cm^{-1} is preferentially enhanced.[36] These Raman bands around 1335 cm^{-1} correspond mainly to stretching modes of various CN bonds of adenine.[37] No relative shift in the positions of RR and SERRS bands was observed. The broad bands located below 1000 cm^{-1} in the RR

dx.doi.org/10.1021/ja210446w | J. Am. Chem.Soc. 2012, 134, 1966−1969

spectrum in Figure 2a are the Raman bands of the fused silica substrate.

Although photoinduced molecular degradation is a major concern in the DUV wavelength range,[38] the incident optical power used here, 0.65 mW, which corresponds to a power density of ~90 kW/cm^2 at the focal spot, allowed the Raman signal to be collected for reasonably long durations (see the SI). For a 1 nm thick adenine layer, we calculated the number of adenine molecules present in the illuminated laser spot to be ~9 amol (see the SI). The Raman signal strength could be improved by a factor of 2−3 by increasing the collection time. Further, since the effective coverage of Al nanoparticles was only 25% and an SNR of 3 is sufficient for analytical detection, we estimate the detection sensitivity of our current system to be ~50 zmol (~30 000 molecules).

We further performed SERRS measurements on nanoparticle arrays with different particle diameters. In Figure 2b, the intensity of the strongest peak (1335 cm^{-1}) is plotted as a function of nanoparticle diameter. It is seen that the SERRS intensity decreased with decreasing nanoparticle diameter and that the signal was smallest for adenine on the bare fused silica substrate. The measured signal was strongly correlated with the position and the strength of the quadrupolar mode, and therefore, the observed signal enhancement can be attributed to the enhanced near-field associated with this resonant mode. In Figure 2c, the peak intensity of the 1335 cm^{-1} adenine band is plotted for Raman measurements made at different positions on nanoparticle arrays and fused silica substrates. The peak intensity remained fairly constant for the individual measurements made on the same substrate. This clearly proves that the analytes can be detected reproducibly with high sensitivity using designed Al nanoparticle arrays as SERRS substrates. In contrast to previous studies claiming similar sensitivity,[39] the high sensitivity in our case was achieved without using any surface functionalization. The reproducibility of the Raman signal on the fused silica substrate also confirmed that adenine was deposited uniformly by the sublimation technique.

We also carried out simulations based on the finite-difference time-domain (FDTD) method to gain insight into the far-field and near-field optical properties of the nanoparticle arrays. As shown in Figure 3c, the nanoparticles were modeled as tapered cylinders with an Al core and a 3 nm thick Al_2O_3 shell. The simulation domain was limited to the unit cell of the nanoparticle array by employing appropriate periodic and absorbing boundary conditions. A uniform square mesh with a pitch of 1 nm was used for discretization of the simulation domain. The Drude−Lorentz model with the optical constants tabulated in ref 14 was used to model the material properties, and a Gaussian pulse was used as the excitation source. As shown in Figure 3a,b, a good overall match between the experimental and simulated plasmon resonance spectra was obtained within the calculated spectral range (200−500 nm).

Optical near-fields were calculated using a plane wave with a wavelength of 257.2 nm and polarization parallel to the substrate plane. The calculated near-field distributions are presented in Figure 3d,e. It can be seen that the EM field intensity ($|\mathbf{E}|^2$) was the highest at the edges of the nanoparticles. The maximum calculated intensity of ~1630, shown as two bright dots in Figure 3e, was achieved on the top edge of the Al core along the polarization axis. However, this was not accessible to the molecules on the surface because of the presence of the oxide shell. The maximum field intensity outside the oxide layer was ~100 and localized at the top

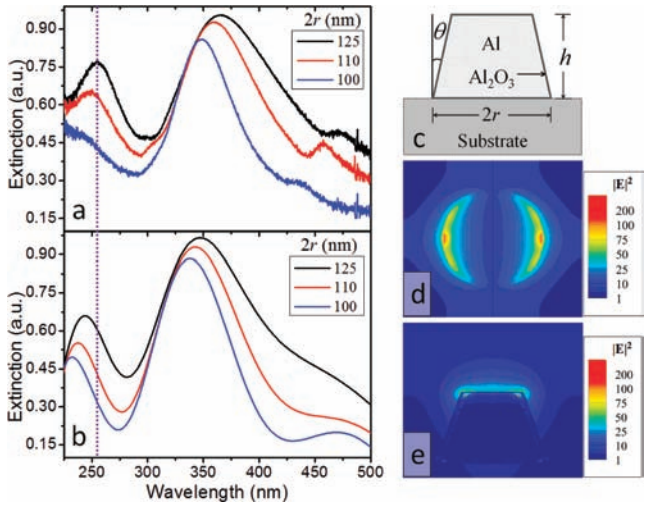

Figure 3. Comparison of (a) experimental and (b) theoretical far-field optical transmission spectra of various nanoparticle arrays. (c) Nanoparticle morphology used for the simulations. The base diameter was 2r, the height (h) 70 nm, the diminution angle (θ) was 12°, and the Al_2O_3 shell thickness was 3 nm. (d) Near-field distribution at 257.2 nm on the top surface (above the oxide shell) of a 140 nm diameter Al nanoparticle. (e) Cross-sectional view of the near-field distributions.

corners of the nanoparticles. Since the EF in SERS scales approximately with $|\mathbf{E}|^4$, the calculations indicate that the maximum EF could be as high as 10^4. Nevertheless this EF would be limited to a highly localized area on the nanoparticle surface, and the average EF was ~850 on the top surface of the nanoparticle. In comparison, we observed that the Raman signal of adenine on nanoparticle arrays with the same diameter was ~13 times higher than that on the bare substrate. Since most of the signal enhancement comes from the top surface of the nanoparticle, which accounts for 25% of the area for the largest nanoparticles, we estimate the average experimental EF to be ~50, a value which is much lower than the calculated one. The difference between the experiment and theory may result from differences between the nanoparticle parameters used for the simulations and those of the fabricated nanoparticle array. The edges of the simulated nanoparticles where most of the field enhancement was localized had a sharpness defined by the pitch of the mesh (i.e., 1 nm). Even if such sharp edges could be produced, they would undergo oxidation,[22] and hence, the nanoparticles would have an effective rounded edge resulting in a lower enhancement. The oxide layer may also be thicker than the assumed value of 3 nm, leading to a further decrease in the EF outside the shell. In addition, the fabricated nanoparticles had a finite roughness due to the crystalline nature of Al, and this effect of roughness is difficult to take into account using the FDTD method. Thus, our simulations provide a good understanding of both the near-field and far-field optical properties of the Al nanoparticles, while simulations with further refinements may yield better correlations between the observed and calculated enhancement factors.

In summary, in this communication we have demonstrated a DUV-SERRS effect resulting from adenine films sublimated on designed Al nanostructures. The signal enhancement results from an increased EM near-field associated with the quadrupolar plasmon resonance modes of the nanoparticle arrays. Less than 10 amol of adenine molecules were detected reproducibly within a collection time of 1 s. The detection sensitivity of the current optical setup is estimated to be

~30 000 adenine molecules. Higher sensitivity could readily be achieved by increasing the collection and detection efficiency of the optical setup, and the detection limit could also be further improved by optimizing the Al nanostructures. Nanoparticle dimers, for example, exhibit extremely high EM enhancements in the interparticle gaps[3] and could give rise to higher EFs. In conclusion, DUV-SERRS promises to be a highly useful analytical technique for ultrasensitive and label-free detection of biomolecules in real time.

■ ASSOCIATED CONTENT

Supporting Information

Details of substrate fabrication, instrumentation, absorption measurements, and SERRS intensity decay measurements. This material is available free of charge via the Internet at http://pubs.acs.org.

■ AUTHOR INFORMATION

Corresponding Author

shankar.jha@mat.ethz.ch; yasin.ekinci@mat.ethz.ch

Present Address

[‖]Biophysics Group, Optical Technology Division, National Institute of Standards and Technology, Gaithersburg, MD 20899, USA.

■ ACKNOWLEDGMENTS

The authors acknowledge the technical help from M. Vockenhuber and T. Mathias. Part of this work was performed at the Swiss Light Source (SLS), Paul Scherrer Institute, Switzerland. M.A. thanks V. Sandoghdar for continuous support and encouragement.

■ REFERENCES

(1) Long, D. A. *The Raman Effect*; Wiley: Chichester, U.K., 2002.
(2) *Surface-Enhanced Raman Scattering*; Kneipp, K., Moskovits, M., Kneipp, H., Eds.; Springer: Berlin, 2006.
(3) Le Ru, E. C.; Etchegoin, P. G. *Principles of Surface-Enhanced Raman Spectroscopy*; Elsevier: Amsterdam, 2009.
(4) Kosuda, K. M.; Bingham, J. M.; Wustholz, K. L.; Van Duyne, R. P. In *Comprehensive Nanoscience and Technology*; Andrews, D. L., Scholes, G. D., Wiederrecht, G. P., Eds.; Academic Press: Oxford, U.K., 2011; Vol. 3.
(5) Kneipp, K.; Wang, Y.; Kneipp, H.; Perelman, L. T.; Itzkan, I.; Dasari, R.; Feld, M. S. *Phys. Rev. Lett.* **1997**, *78*, 1667.
(6) Nie, S. M.; Emery, S. R. *Science* **1997**, *275*, 1102.
(7) Blackie, E. J.; Le Ru, E. C.; Etchegoin, P. G. *J. Am. Chem. Soc.* **2009**, *131*, 14466.
(8) Efremov, E. V.; Ariese, F.; Gooijer, C. *Anal. Chim. Acta* **2008**, *606*, 119.
(9) Asher, S. A.; Johnson, C. R. *Science* **1984**, *225*, 311.
(10) Asher, S. A. *Anal. Chem.* **1993**, *65*, 59A.
(11) Fodor, S. P. A.; Spiro, T. G. *J. Am. Chem. Soc.* **1986**, *108*, 3198.
(12) Neugebauer, U.; Schmid, U.; Baumann, K.; Holzgrabe, U.; Ziebuhr, W.; Kozitskaya, S.; Kiefer, W.; Schmitt, M.; Popp, J. *Biopolymers* **2006**, *82*, 306.
(13) (a) Ahmed, Z.; Beta, I. A.; Mikhonin, A. V.; Asher, S. A. *J. Am. Chem. Soc.* **2005**, *127*, 10943. (b) Ahmed, Z.; Myshakina, N. S.; Asher, S. A. *J. Phys. Chem. B* **2009**, *113*, 11252.
(14) *Handbook of Optical Constants of Solids*; Palik, E. D., Ghosh, G., Eds.; Academic Press: San Diego, CA, 1998.
(15) Lin, X. F.; Ren, B.; Yang, Z.-L.; Liu, G. K.; Tian, Z.-Q. *J. Raman Spectrosc.* **2005**, *36*, 606.
(16) Ren, B.; Lin, X. F.; Yang, Z. L.; Liu, G. K.; Aroca, R. F.; Mao, B. W.; Tian, Z. Q. *J. Am. Chem. Soc.* **2003**, *125*, 9598.
(17) Tian, Z.-Q.; Yang, Z. L.; Ren, B.; Wu, D. Y. In *Surface-Enhanced Raman Scattering*; Kneipp, K., Moskovits, M., Kneipp, H., Eds.; Springer: Berlin, 2006.
(18) Borodko, Y.; Humphrey, S. M.; Tilley, T. D.; Frei, H.; Somorjai, G. A. *J. Phys. Chem.* **2007**, *111*, 6288.
(19) Xu, L.; Fang, Y. *Spectrochim. Acta, Part A* **2005**, *61*, 1991.
(20) Ekinci, Y.; Solak, H. H.; Löffler, J. F. *J. Appl. Phys.* **2008**, *104*, No. 083107.
(21) Langhammer, C.; Schwind, M.; Kasemo, B.; Zoric, I. *Nano Lett.* **2008**, *8*, 1461.
(22) Chen, G. H.; Zhao, J.; Schatz, G. C.; Van Duyne, R. P. *J. Phys. Chem. C* **2008**, *112*, 13958.
(23) Mohammadi, A.; Sandoghdar, V.; Agio, M. *J. Comput. Theor. Nanosci.* **2009**, *6*, 2024.
(24) Jeyaram, Y.; Jha, S. K.; Agio, M.; Löffler, J. F.; Ekinci, Y. *Opt. Lett.* **2010**, *35*, 1656.
(25) Chowdhury, M. H.; Ray, K.; Gray, S. K.; Pond, J; Lakowicz, J. R. *Anal. Chem.* **2009**, *81*, 1397.
(26) Dörfer, T.; Schmitt, M.; Popp, J. *J. Raman Spectrosc.* **2007**, *38*, 1379.
(27) Taguchi, A.; Hayazawa, N.; Furusawa, K.; Ishitobi, H.; Kawata, S. *J. Raman Spectrosc.* **2009**, *40*, 1324.
(28) Yang, Z.-L.; Li, Q.-H.; Ren, B.; Tian, Z.-Q. *Chem. Commun.* **2011**, *47*, 3909.
(29) Sun, M.; Zhang, S.; Fang, Y.; Yang, Z.; Wu, D.; Dong, B.; Xu, H. *Appl. Phys. Lett.* **2001**, *78*, 802.
(30) Yang, Z.; Li, Q.; Fang, Y.; Sun, M. *Chem. Commun.* **2011**, *47*, 9131.
(31) Päivänranta, B.; Langner, A.; Kirk, E.; David, C.; Ekinci, Y. *Nanotechnology* **2011**, *22*, No. 375302.
(32) Du, H.; Fuh, R. A.; Li, J.; Corkan, A.; Lindsey, J. S. *Photochem. Photobiol.* **1998**, *68*, 141.
(33) Middleton, C. T.; de La Harpe, K.; Su, C.; Law, Y. K.; Crespo-Hernández, C. E.; Kohler, B. *Annu. Rev. Phys. Chem.* **2009**, *60*, 217.
(34) Barbatti, M.; Aquino, A. J. A.; Lischka, H. *Phys. Chem. Chem. Phys.* **2010**, *12*, 4959.
(35) Yamada, T.; Fukutome, H. *Biopolymers* **1968**, *6*, 43.
(36) Chen, T. T.; Liang, N. T.; Huang, H. J.; Chou, Y .C. *Chin. J. Phys.* **1987**, *25*, 205.
(37) Giese, B.; McNaughton, D. *J. Phys. Chem. B* **2002**, *106*, 101.
(38) Kumamoto, Y.; Taguchi, A.; Smith, N. I.; Kawata, S. *Biomed. Opt. Express* **2011**, *2*, 927.
(39) Rodríguez-Lorenzo, L.; Álvarez-Puebla, R. A.; Pastoriza-Santos, I.; Mazzucco, S.; Stéphan, O.; Kociak, M.; Liz-Marzán, L. M.; García de Abajo, F. J. *J. Am. Chem. Soc.* **2009**, *131*, 4616.